Journal of Alloys and Compounds 509 (2011) 7529–7531

Contents lists available at ScienceDirect

Journal of Alloys and Compounds

journal homepage: www.elsevier.com/locate/jallcom

A novel method to synthesis magnetic thin film of iron oxide

R.K. Gupta[a,*], K. Ghosh[a], R. Patel[b], P.K. Kahol[a]

[a] Department of Physics, Astronomy, and Materials Science, Missouri State University, Springfield, MO 65897, USA
[b] Roy Blunt Jordan Valley Innovation Center, Missouri State University, Springfield, MO 65806, USA

ARTICLE INFO

Article history:
Received 15 January 2011
Received in revised form 20 April 2011
Accepted 21 April 2011
Available online 30 April 2011

Keywords:
Iron oxide
Pulsed laser deposition
Magnetization
Superparamagnetic

ABSTRACT

A novel method is used to deposit iron oxide thin film. Frozen iron acetate is used as a target for pulsed laser deposition of iron oxide thin film. KrF excimer laser having wavelength of 248 nm with pulsed duration of 20 ns is used to deposit the film. Structural characterizations were performed using X-ray diffraction and atomic/magnetic force microscopy. The X-ray diffraction patterns confirmed the polycrystalline nature of α-Fe_2O_3. Temperature dependence magnetic measurements in zero field cooled showed the presence of blocking temperature at ~60 K. The magnetic measurements revealed the existence of superparamagnetic behavior above blocking temperature and freezing of magnetic moments arising from uncompensated surface spins below blocking temperature.

1. Introduction

Different forms of iron oxide such as magnetite (Fe_3O_4), maghemite (γ-Fe_2O_3), and hematite (α-Fe_2O_3) are technologically very important [1,2]. They are of interest for various applications such as abrasives, polishing agent, catalyst, gas sensors, pigments, photo anodes, anodes for Li-ion battery, tunneling magnetoresistance based devices, etc. [3–5]. Growth of high quality thin films of iron oxide has received considerable attention because of its technological applications in heterogeneous catalysis, magnetic recording, supercapacitor, and integrated microwave devices [6,7].

Pulsed laser deposition technique (PLD) is an effective method to produce high quality thin films due to the high kinetic energy of atoms and ionized species in the laser-produced plasma [8]. Bollero et al. [9] had used PLD for deposition of Fe_3O_4 thin films. Thin films of iron oxide with columnar growth of iron oxide grains were deposited using sputtering technique [10]. α-Fe_2O_3 thin films were grown using chemical vapor deposition technique with the source material of $Fe(CO)_5$ [11]. It was observed that α-Fe_2O_3 phase was more stable in the low temperature range, while Fe_3O_4 phase was observed above 120 °C. Lie et al. [12] have utilized atomic layer deposition technique for deposition of Fe_2O_3 thin films with $Fe(thd)_3$ (iron derivative of thd = 2,2,6,6-tetramethylheptane-3,5-dione) and ozone as precursors. Gich et al. [13] have grown epitaxial thin films of Fe_2O_3 on strontium titanate. Recently, we have fabricated highly conducting, transparent, and ferromagnetic multilayers thin films based on ZnO and Fe_3O_4 using PLD [14].

In this letter, we report a novel method for deposition of iron oxide thin film using PLD. We have used a frozen target of iron acetate instead of solid iron oxide target for ablation in PLD. The structural and magnetic properties were studied using X-ray diffraction (XRD), atomic/magnetic force microscopy (A/MFM) and superconducting quantum interference device (SQUID) magnetometer.

2. Experimental details

Iron acetate (FeAc) was obtained from Alfa Aesar (USA). The starting solution was prepared by dissolving 1.0 g of the FeAc in 10 ml of deionized water. The solution was poured into a target cup, cooled to liquid nitrogen temperature, and kept in the liquid nitrogen bath for 20 min. The frozen target was then installed inside a vacuum chamber evacuated to ~10^{-5} mbar. KrF excimer laser pulses (Lambda Physik COMPex, λ = 248 nm; pulse duration of 20 ns) at a pulse rate of 10 Hz and fluence of 300 mJ/pulses were directed at a 45° angle of incidence on the frozen target. The target was rotated with a constant speed to avoid excessive heating and erosion of a single spot on the frozen target. Sapphire was used as substrate.

The structural characterizations were performed using X-ray diffraction and atomic force microscopy. The XRD spectrum of the film was recorded with Bruker AXS X-ray diffractometer using the 2θ–θ scan with CuKα (λ = 1.5405 Å) radiation, which operated at 40 kV and 40 mA. Atomic force microscopy and magnetic force microscopy imaging were performed under ambient conditions using a Digital Instruments (Veeco) Dimension-3100 unit with Nanoscope® III controller, operated in tapping mode. The optical transmittance measurements were made using UV–visible spectrophotometer (Ocean Optics HR4000). The thickness of the film was measured using Dektak 150 Surface Profiler and estimated to be 80 nm. Quantum Design MPMS XL-T superconducting quantum interference device (SQUID) magnetometer was used to study the magnetic properties.

* Corresponding author. Tel.: +1 417 8366298; fax: +1 417 8366226.
E-mail address: ramguptamsu@gmail.com (R.K. Gupta).

0925-8388/$ – see front matter © 2011 Elsevier B.V. All rights reserved.
doi:10.1016/j.jallcom.2011.04.118

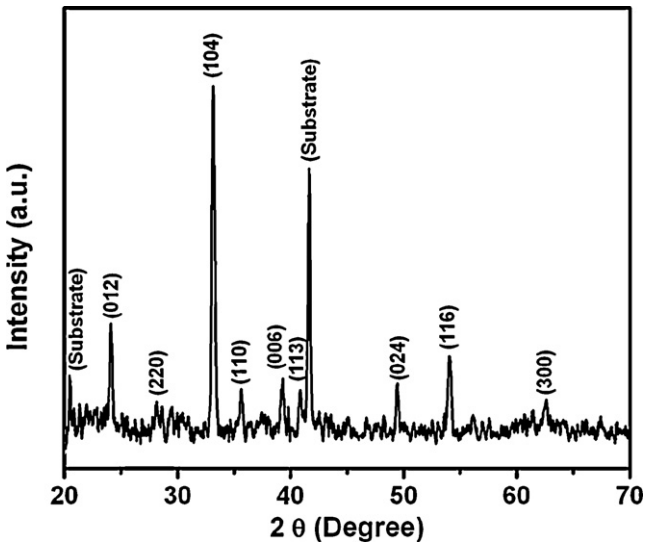

Fig. 1. XRD patterns of iron oxide thin film.

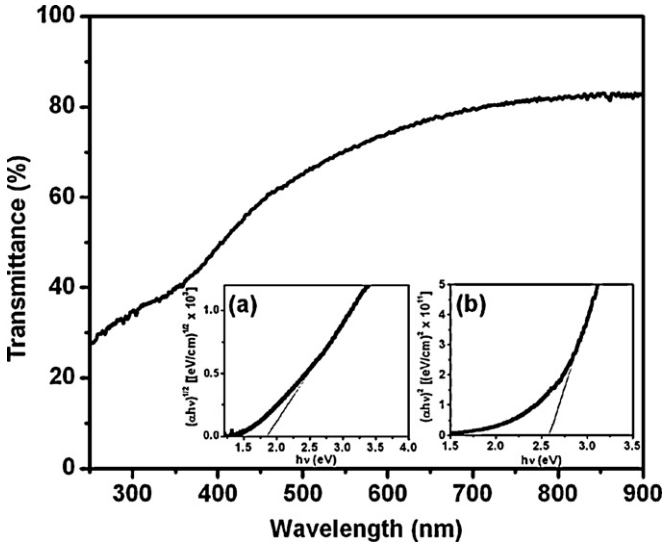

Fig. 2. UV–visible spectra of iron oxide thin film (inset figure shows (a) indirect and (b) direct bandgap).

3. Results and discussion

The X-ray diffraction patterns of thin film deposited on sapphire substrate is shown in Fig. 1. The film shows polycrystalline nature. All of the observed peaks of the X-ray diffraction patterns in Fig. 1 can be indexed to α-Fe_2O_3 (JCPDS No. 86-0550). No other impurities were observed.

The transmittance spectra of the film are shown in Fig. 2. The optical band gap of the film is calculated from the transmittance versus wavelength spectra. The absorption coefficient (α) is calculated using the equation

$$\alpha = \ln \frac{(1/T)}{d} \quad (1)$$

where T is transmittance and d is film thickness. The absorption coefficient (α) and the incident photon energy ($h\nu$) is related by the following equation [15]

$$(\alpha h\,\nu)^n = A(h\nu - E_g) \quad (2)$$

where A and E_g are constant and optical band gap, respectively. n is 1/2 or 2 for indirect or direct bandgap semiconductor respectively. The E_E can be determined by extrapolations of the linear portion of the curve to the $h\nu$ axis. The inset of Fig. 2 shows the curves of $(\alpha h\nu)^n$ versus photon energy. The direct and indirect band gaps are found to be 2.6 and 1.8 eV respectively. The published data confirmed that the bandgap of α-Fe_2O_3 is ranging from 2.4 to 2.7 eV depending on deposition method and conditions [16,17]. It is also observed that the quality, purity, and structure of the deposited films could also affect the bandgap.

Fig. 3 shows the AFM (left image) and corresponding MFM magnetic domain (right image) patterns of the same area of film for better comparison. AFM image shows the presence of small grains. The presence of magnetic domain due to grains of iron oxide is quite evident in MFM image. The grain size of the film is about 65 nm. The root mean square (rms) surface roughness of the film is estimated to be 26 nm. The MAPLE grown film has large grain size compared to the film grown using atomic layer deposition (ALD). The ALD grown film showed grain size of about 45 nm [18].

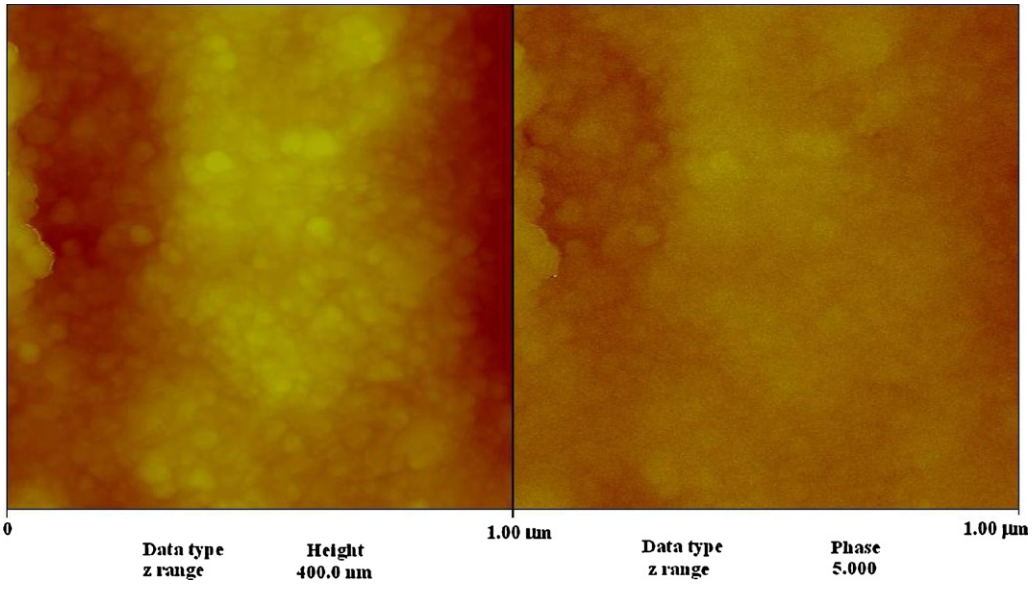

Fig. 3. AFM (left image) and MFM (right image) images of iron oxide thin film.

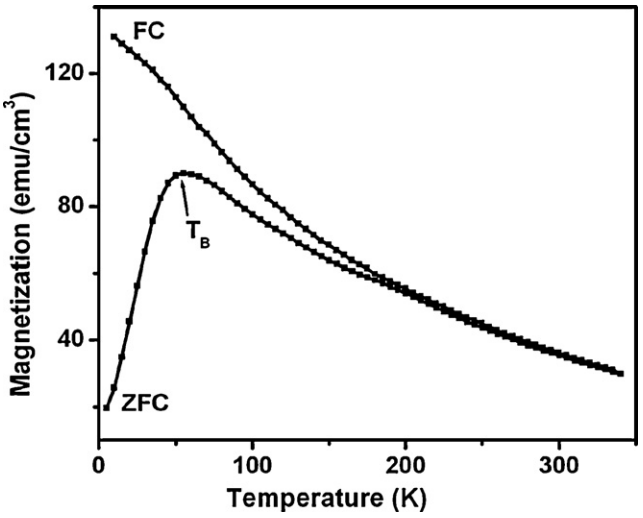

Fig. 4. ZFC and FC temperature dependent magnetization curves for iron oxide thin film.

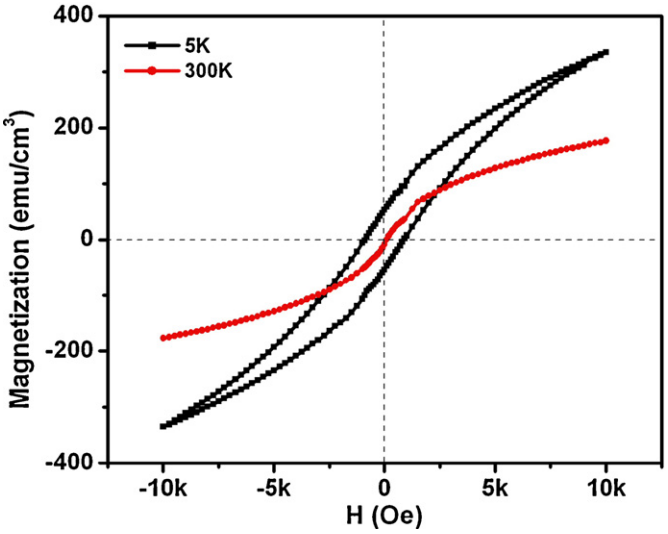

Fig. 5. Hysteresis loop of iron oxide thin film measured at different temperatures.

The temperature dependence of magnetization in regimes of zero-field-cool (ZFC) and FC in applied dc field of 500 Oe (Oersted) is shown in Fig. 4. ZFC magnetization curve rapidly increases with increase in temperature upto ~60 K and than decreases with increase in temperature. On the other hand, the FC magnetization curve shows continuous decrease in magnetization with temperature. At high temperature, i.e. above the blocking temperature ZFC and FC magnetization data exhibit a similar trend. The magnetization maximum in ZFC is related with the blocking temperature (T_B). The presence of maximum and irreversibility of ZFC and FC curves indicate that above blocking temperature iron oxide is characterized by superparamagnetic behavior, whereas below blocking temperature the magnetic moment of iron oxide is frozen in local field direction [19]. Since the T_B indicates the threshold point of thermal activation, the magnetocrystalline anisotropy of the iron oxide is overcome by thermal activation starting at T_B and the magnetization direction of each iron oxide particle simply follows the applied direction. Consequently, the iron oxide nanocrystals show super paramagnetic properties. Further, the magnetic anisotropy blocks the change of magnetization direction below T_B, a certain magnetic field is required to change the magnetic direction, therefore, the iron oxide nanoparticles show coercivity and hysteric behavior [20].

To further confirm the freezing process below blocking temperature and superparamagnetic behavior above blocking temperature, we study field dependence magnetization at 5 K and 300 K. Fig. 5 shows the variation of magnetization as a function of magnetic field (M–H) under different constant temperatures. M–H measurement at 5 K clearly shows the presence of hysteresis loop indicating the ferromagnetic behavior of the film. The coercivity field is ~820 Oe at 5 K. The M–H plot at 300 K does not show any hysteresis and we observe a decrease in magnetization. The non-existence of coercivity and decrease in saturation magnetization clearly indicates the superparamagnetic behavior.

4. Conclusions

In summary, a novel method was used for deposition of iron oxide thin film using frozen iron acetate as a target in pulsed laser deposition. The deposited film was polycrystalline in nature. The magnetic measurement showed the presence of blocking temperature at ~60 K. The presence of blocking temperature and non-irreversibility of zero field cool and field cool magnetization confirmed the superparamagnetic behavior. The film showed hysteresis in field dependence magnetization measurement at 5 K, which vanished above blocking temperature.

Acknowledgments

Authors are thankful to Prof. R. Mayanovic, Missouri State University, for providing XRD facility.

References

[1] A.S. Teja, P.Y. Koh, Prog. Cryst. Growth Charact. Mater. 55 (2009) 22.
[2] G. Wu, X. Tan, G. Li, C. Hu, J. Alloys Compd. 504 (2010) 371.
[3] G. Tong, W. Wu, J. Guan, H. Qian, J. Yuan, W. Li, J. Alloys Compd. 509 (2011) 4320.
[4] G.Y. Zhang, Y.Y. Xu, D.Z. Gao, Y.Q. Sun, J. Alloys Compd. 509 (2011) 885.
[5] H. Liu, D. Wexler, G. Wang, J. Alloys Compd. 487 (2009) L24.
[6] Y. Gao, S.A. Chambers, J. Cryst. Growth 174 (1997) 446.
[7] P.M. Kulal, D.P. Dubal, C.D. Lokhande, V.J. Fulari, J. Alloys Compd. 509 (2011) 2567.
[8] R.K. Gupta, K. Ghosh, S.R. Mishra, P.K. Kahol, Appl. Surf. Sci. 254 (2008) 4018.
[9] A. Bollero, M. Ziese, R. Hohne, H.C. Semmelhack, U. Kohler, A. Setzer, P.J. Esquinazi, Magn. Magn. Mater. 285 (2005) 279.
[10] Y. Peng, C. Park, D.E. Laughlin, J. Appl. Phys. 93 (2003) 7957.
[11] E.T. Lee, B.J. Kim, J.E. Jang, Thin Solid Films 341 (1999) 73.
[12] M. Lie, H. Fjellvag, A. Kjekshus, Thin Solid Films 488 (2005) 74.
[13] M. Gich, J. Gazquez, A. Roig, A. Crespi, J. Fontcuberta, J.C. Idrobo, S.J. Pennycook, M. Varela, V. Skumryev, M. Varela, Appl. Phys. Lett. 96 (2010) 112508.
[14] R.K. Gupta, K. Ghosh, P.K. Kahol, Mater. Lett. 64 (2010) 1487.
[15] V.R. Shinde, T.P. Gujar, C.D. Lokhande, R.S. Mane, S.H. Han, Mater. Chem. Phys. 96 (2006) 326.
[16] R.A. Ismail, Y. Najim, M. Ouda, e-J. Surf. Sci. Nanotechnol. 6 (2008) 96.
[17] A. Watanabe, H. Kozuka, J. Phys. Chem. B 107 (2003) 12713.
[18] O. Nilsen, M. Lie, S. Foss, H. Fjellvay, A. Kjekshus, Appl. Surf. Sci. 227 (2004) 40.
[19] A. Zelenakova, J. Kovac, V. Zelenak, Acta. Phys. Pol. A 115 (2009) 357.
[20] Z.L. Wang, Y. Liu, Z. Zhang, Handbook of Nanophase and Nanostructured Materials, Vol. 2, Kluwer Academic Publishers, 2002.